

**Supporting Information for
Compositional variability of San Carlos olivine**

S. Lambert¹, S. Hamilton¹, and O. Lang^{1,2}

¹Department of Geology and Geophysics, University of Utah.

²Department of Geography, University of Utah.

Contents of this file: Figures S1 to S6 and references cited in Supplementary Figures and Supplementary Tables

Additional Supporting Information (Files uploaded separately): Tables S1 to S5

Supplementary Figures.

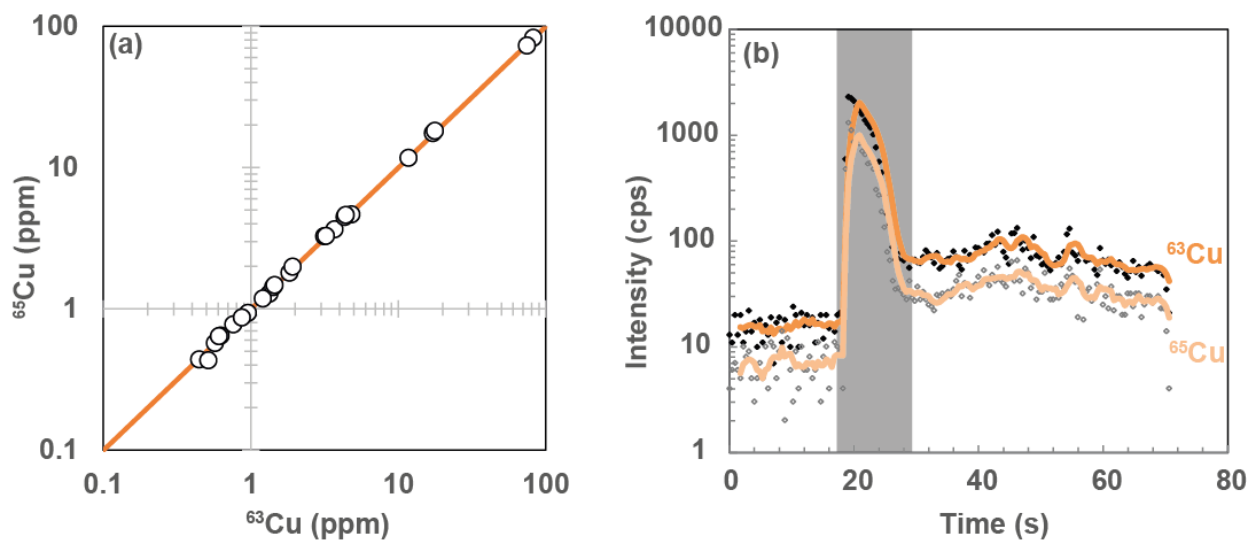


Figure S1. (a) Comparison between the average concentration in copper before correction obtained for olivine analyses performed on xenoliths using ^{63}Cu and ^{65}Cu . (b) Example of signal obtained for ^{63}Cu and ^{65}Cu showing a peak of intensity at the beginning of the line (sample: SC3-2). The shaded area shows the discarded part of the signal to correct for the presence of the inclusion. Note the log-scale on the intensity axis.

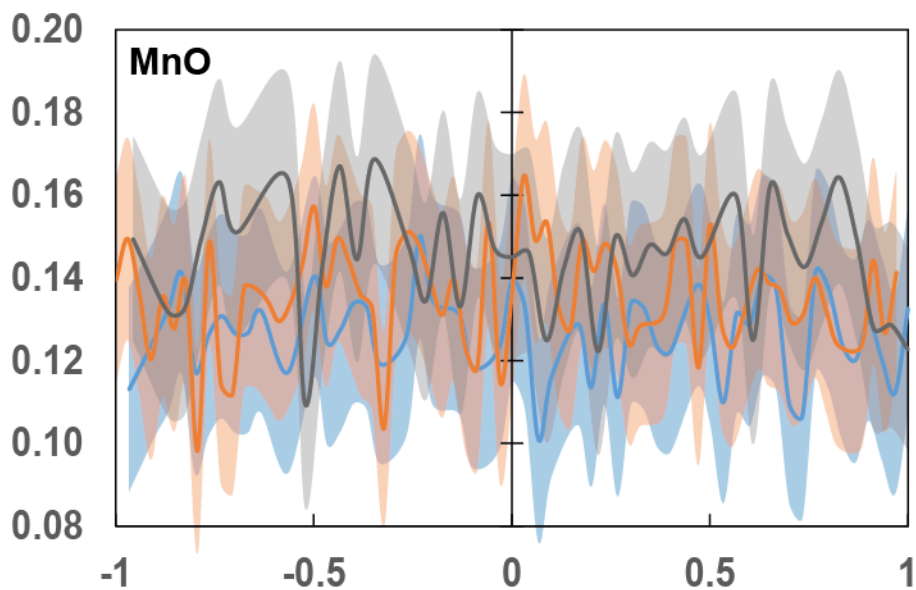


Figure S2. MnO (wt. %) profiles in three large San Carlos grain (non-USNM distributed) using the one-step setup. Distance is normalized to compare the three grains. Spatial resolution is $100\mu\text{m}$. The shaded area around each profile represents $\pm 2\text{AE}$.

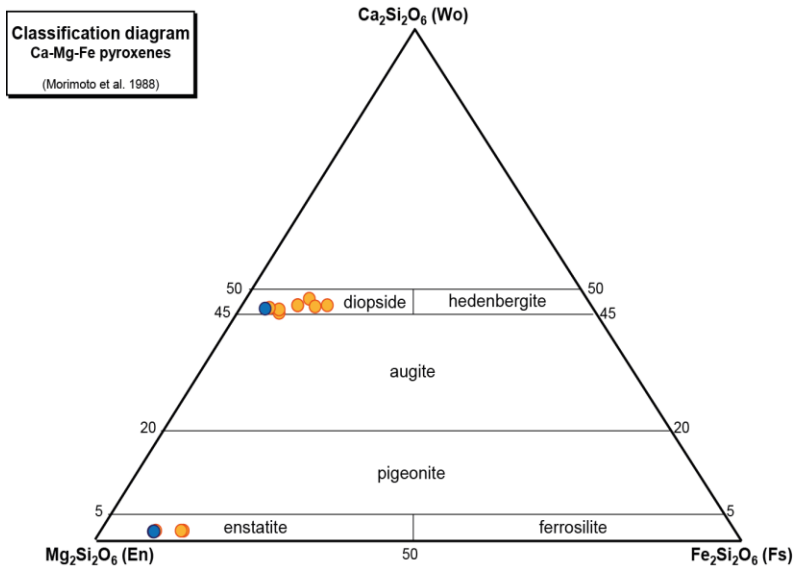


Figure S3. Compositions of the clinopyroxenes analyzed in this study (yellow: pyroxenite; blue: peridotite). Diagram was built with PX-NOM (Sturm, 2002).

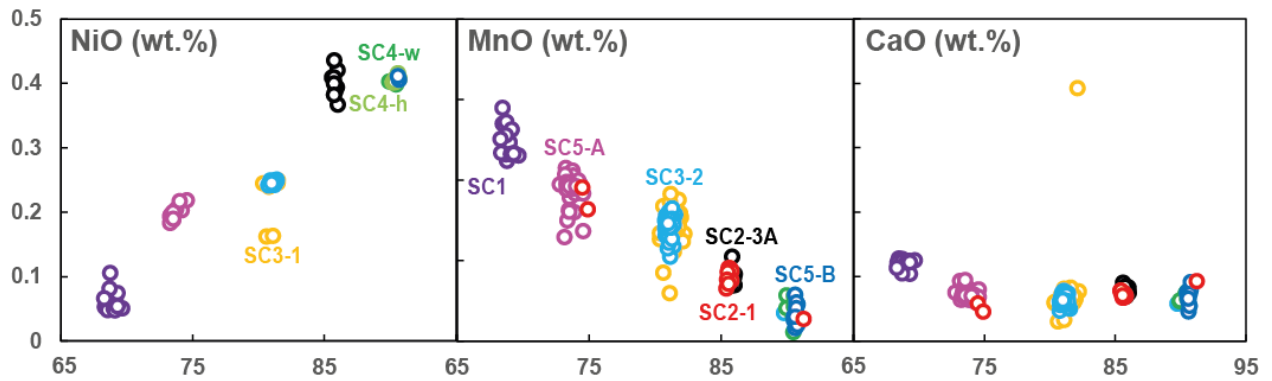


Figure S4. Minor elements concentrations in the olivines from the xenoliths. Both 1-step and two-step analyses are represented.

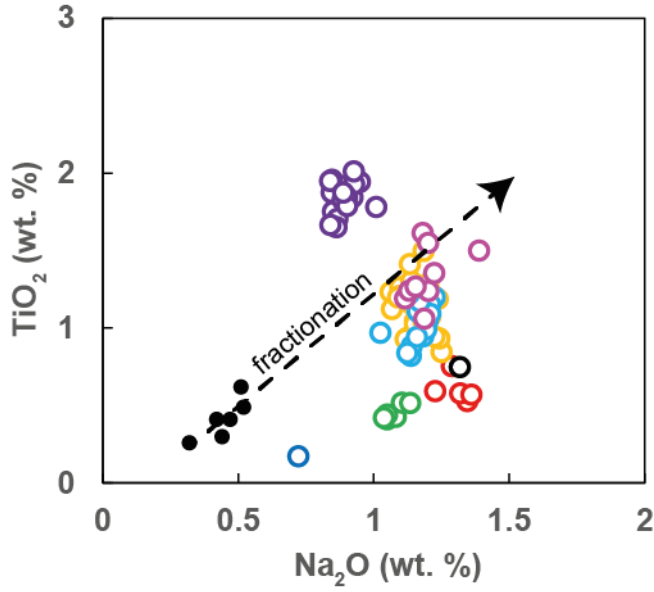


Figure S5. TiO₂ vs Na₂O in clinopyroxene analyzed in this study (open circles) compared with the extrapolation trend obtained from the clinopyroxenes (black circles) along the liquid line of descent of a tholeiitic basalt during equilibrium crystallization at 1 GPa (Villiger et al., 2004). The color code is the same than in Figure S3.

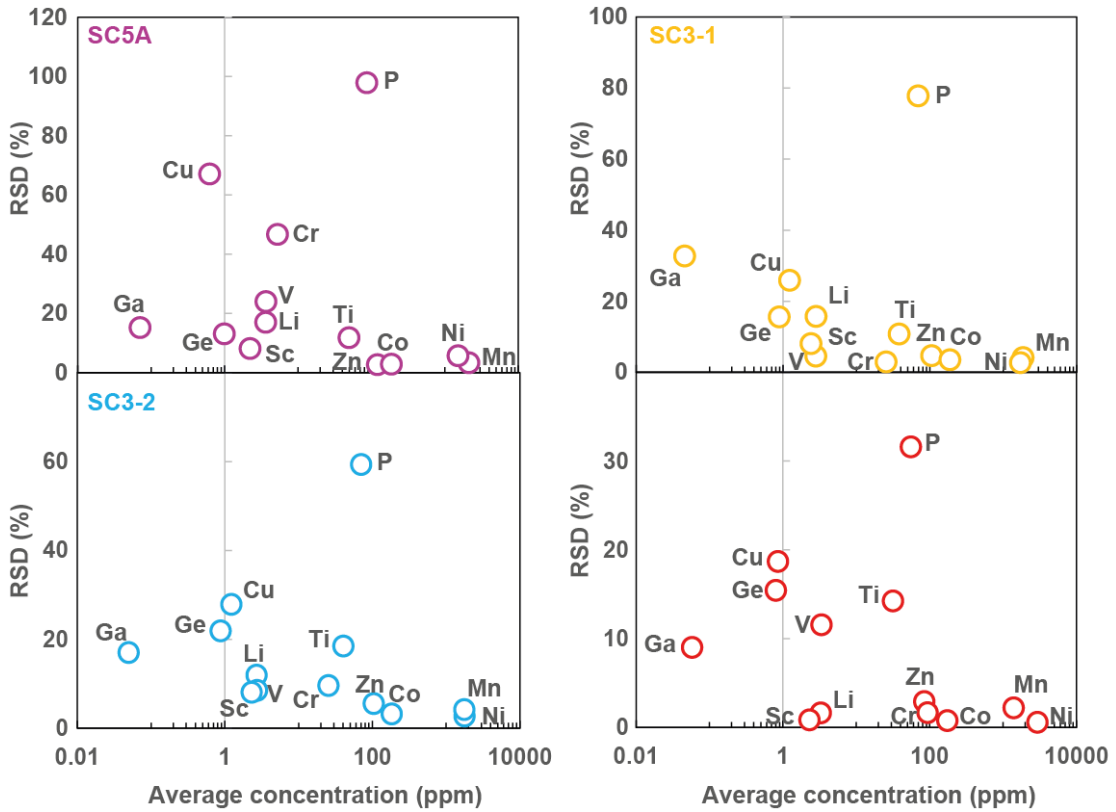


Figure S6. Relative variability ($RSD=2SD/\text{Average concentration}$) of the trace and minor element concentrations in the olivine for the xenoliths SC5-A, SC3-1, SC3-2 and SC2-1.

Supplementary references:

- Batanova, V. G., Sobolev, A. V., & Kuzmin, D. V. (2015). Trace element analysis of olivine: High precision analytical method for JEOL JXA-8230 electron probe microanalyser. *Chemical Geology*, 419, 149-157.
- Batanova, V. G., Thompson, J. M., Danyushevsky, L. V., Portnyagin, M. V., Garbe-Schönberg, D., Hauri, E., ... & Sobolev, A. V. (2019). New olivine reference material for in situ microanalysis. *Geostandards and Geoanalytical Research*, 43(3), 453-473.
- Couperthwaite, F. K., Thordarson, T., Morgan, D. J., Harvey, J., & Wilson, M. (2020). Diffusion timescales of magmatic processes in the Moinui lava eruption at Mauna Loa, Hawaii, as inferred from bimodal olivine populations. *Journal of Petrology*, 61(7), ega058.
- De Hoog, J. C., Gall, L., & Cornell, D. H. (2010). Trace-element geochemistry of mantle olivine and application to mantle petrogenesis and geothermobarometry. *Chemical Geology*, 270(1-4), 196-215.
- Gao, S., Liu, X., Yuan, H., Hattendorf, B., Günther, D., Chen, L., & Hu, S. (2002). Determination of forty two major and trace elements in USGS and NIST SRM glasses by laser ablation-inductively coupled plasma-mass spectrometry. *Geostandards Newsletter*, 26(2), 181-196.
- Gordeychik, B., Churikova, T., Kronz, A., Sundermeyer, C., Simakin, A., & Wörner, G. (2018). Growth of, and diffusion in, olivine in ultra-fast ascending basalt magmas from Shiveluch volcano. *Scientific reports*, 8(1), 1-15.
- Li, X., Zeng, Z., Dan, W., Yang, H., Wang, X., Fang, B., & Li, Q. (2020). Source lithology and crustal assimilation recorded in low $\delta^{18}\text{O}$ olivine from Okinawa Trough, back-arc basin. *Lithos*, 360, 105444.
- Lynn, K. J., Garcia, M. O., & Shea, T. (2020). Phosphorus coupling obfuscates lithium geospeedometry in olivine. *Frontiers in Earth Science*, 8, 135.
- Stead, C. V., Tomlinson, E. L., Kamber, B. S., Babechuk, M. G., & McKenna, C. A. (2017). Rare earth element determination in olivine by laser ablation-quadrupole-ICP-MS: An analytical strategy and applications. *Geostandards and Geoanalytical Research*, 41(2), 197-212.
- Sturm, R. (2002). PX-NOM—an interactive spreadsheet program for the computation of pyroxene analyses derived from the electron microprobe. *Computers & Geosciences*, 28(4), 473-483.
- USGS (2002) Geochemical Reference Materials and Certificates.
http://minerals.cr.usgs.gov/geo_chem_stand/
- Villiger, S., Ulmer, P., Müntener, O., & Thompson, A. B. (2004). The liquid line of descent of anhydrous, mantle-derived, tholeiitic liquids by fractional and equilibrium crystallization—an experimental study at 1·0 GPa. *Journal of Petrology*, 45(12), 2369-2388.